

Analysis of Flow Behaviors in Sparger and its Upstream Piping System

3 1370

19

가 가 IRWST(In-containment Refueling Water Storage Tank)
reducer, expander, 90° elbow
sparger
Sparger
sparger
Sparger sparger header
sparger IRWST
sparger IRWST

Abstract

The In-containment Refueling Water Storage Tank (IRWST) has the function of heat sink when steam is released from the pressurizer. The steam having high pressure and temperature pass through various type of tubes, such as reducer, expander, and 90° elbow etc., and finally discharged into condensation pool through spargers submerged into it. The hydrodynamic behaviors occurring at the sparger are very complex because of the wide variety of operating conditions and the complex geometry. Hydrodynamic behavior when air is discharged through a sparger in a condensation pool is investigated using CFD techniques in the present study. The effect of pressure acting on the sparger header during both water and air discharge through the sparger is studied. In addition, pressure oscillation occurring during air discharge through the sparger is studied for a better understanding of

mechanisms of air discharge and a better design of the IRWST, including sparger.

1.

(IRWST: In-containment Refueling Water Storage Tank) (safety injection system) (containment spray system) 가 (heat sink) POSRV(Pilot Operated Safety Relief Valve) IRWST sparger (condensation pool) POSRV 가 sparger (core parts) 가 Sparger (phase change)가 / [1-5]. 가 (group) (coalescence) (breakup) [6-7]. , Tiselj and Petelin[8] sparger POSRV RELAP5 1 , sparger Sparger sparger header IRWST (pressure oscillation)

2.

POSRV 가 가 , (valve opening time) ,

(diaphragm) 가 shock tube
 Shock tube (exact solution)가 가

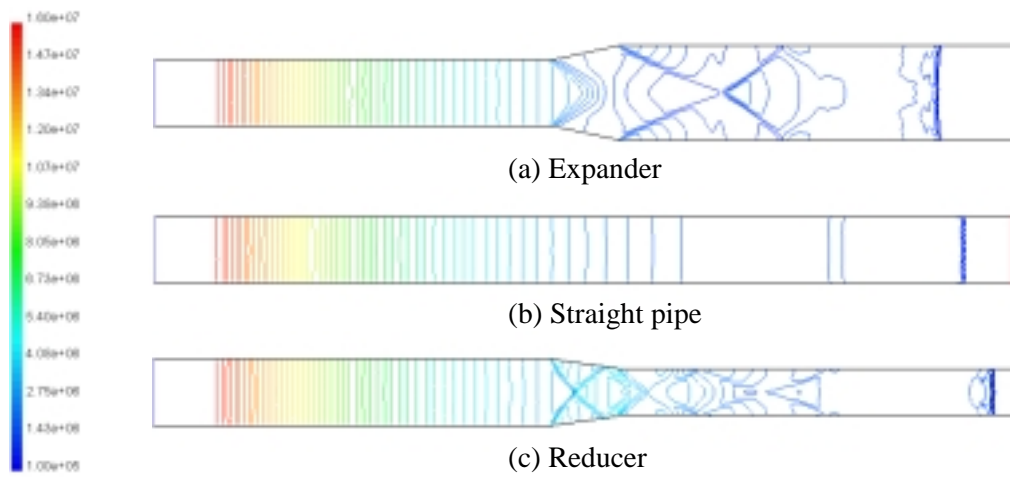


Fig. 1 Pressure distribution

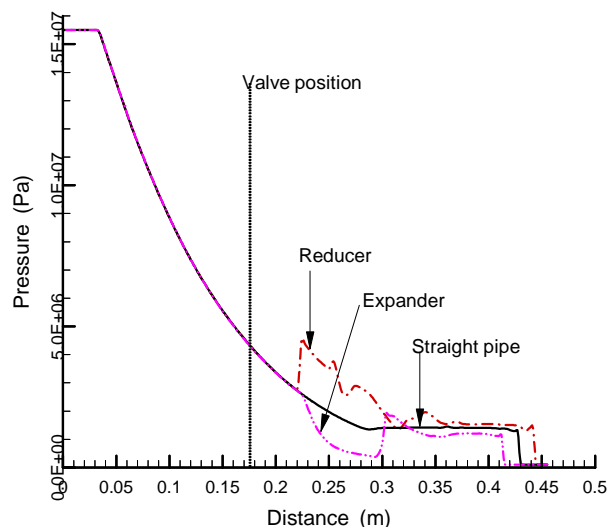


Fig. 2 Pressure distribution, $P_{\text{driver}} = 15,508,929 \text{ Pa}$, $P_{\text{driven}} = 101,325 \text{ Pa}$, Time = 0.0002 sec.

POSRV

reducer

expander

153

1

Figure 1

(expansion wave)

(shock wave)가
wave)가

(normal shock

Figure 2

Reducer expander

가

expander

reducer

90° elbow

90° elbow

2

3

2

3

가

90° elbow

Figure 3

90° elbow

35 mm

70 mm

POSRV 가

가

POSRV

10

1

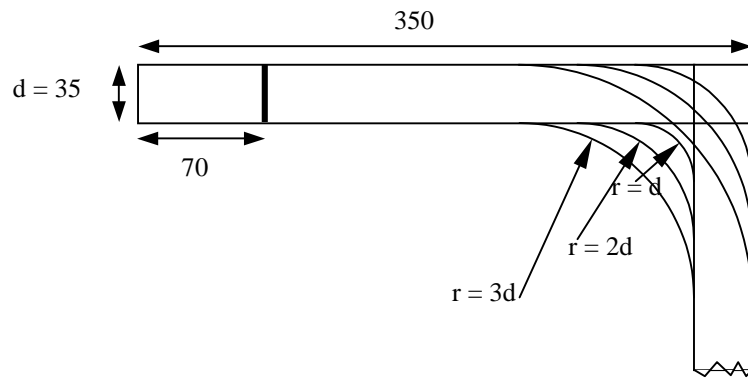


Fig. 3 Outline of the 90° elbow.

Figure 4

zero(r = 0)

90° elbow

2

3

2

3

가

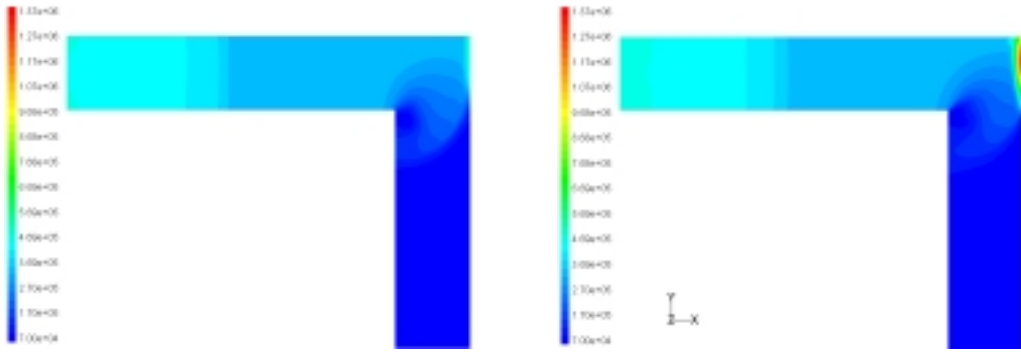
1

가

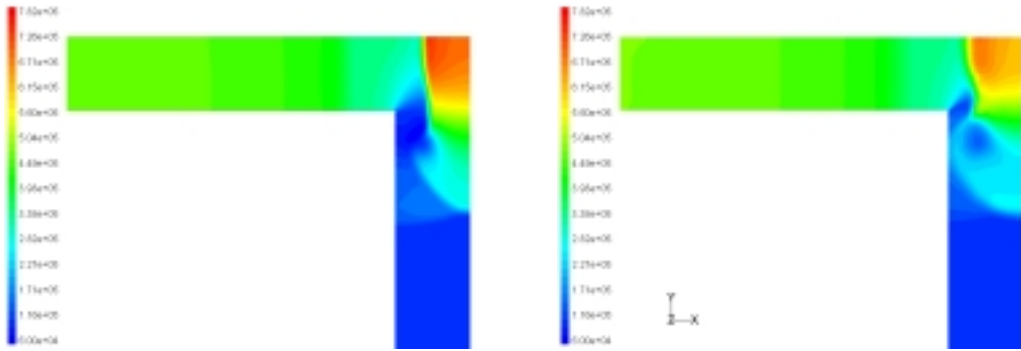
90° elbow

90° elbow

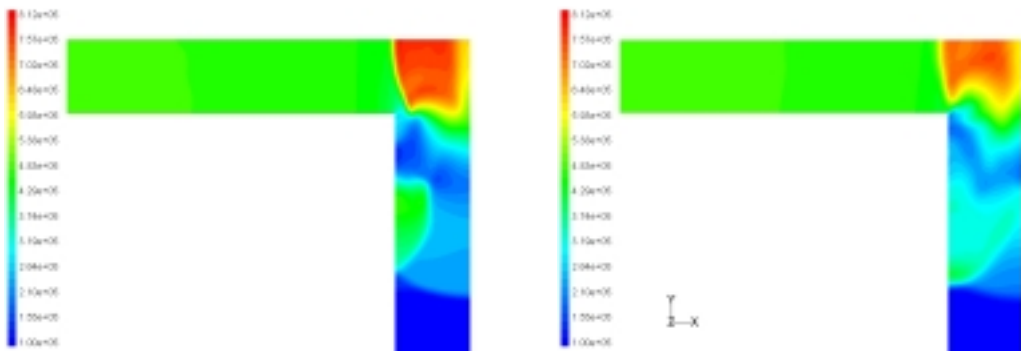
1



(a) Time = 0.000469 sec



(b) Time = 0.000537 sec



(c) Time = 0.000611 sec

Fig. 4 Pressure distribution in a 90° elbow (LHS = 2-d analysis, RHS = 3-d analysis).

2 3 x-

가 가 (sonic

velocity) 가 90° elbow

가 , 가 가

(dynamic pressure)

가

가

90° elbow

Figure 5 90° elbow x-

2

3

가

Figure 6

3

가

90° elbows

x-

x-

1

1

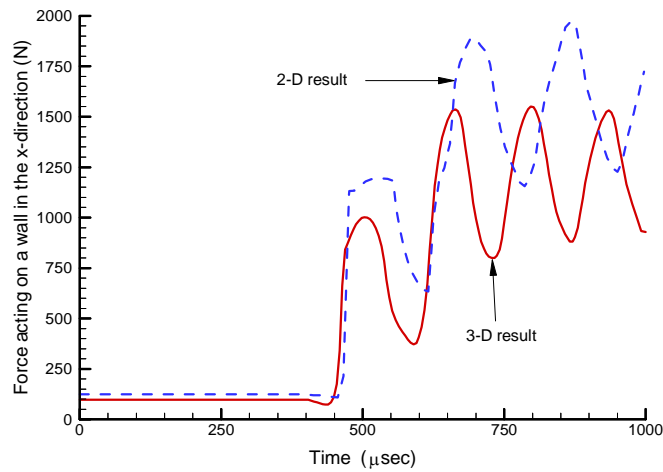


Fig. 5 Force acting on the wall in the x-direction for a 90° elbow having a zero of radius at the corner.

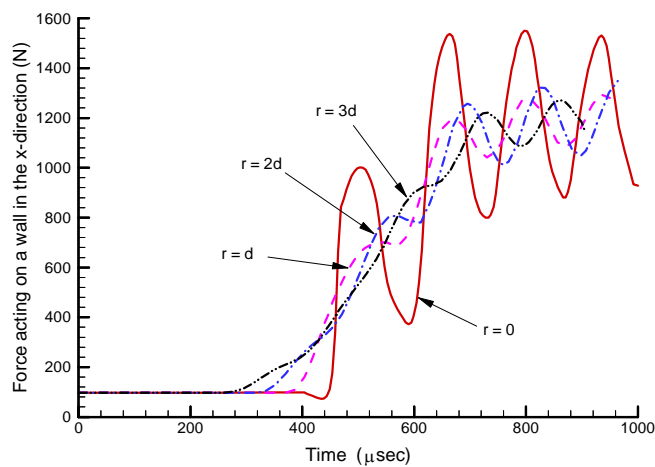


Fig. 6 Comparison of force acting on the wall in the x-direction for 90° elbows having different radii at the corner.

3. VOF

Hirt et al.⁽⁹⁾ 2 (two-phase flow)
 VOF(Volume of Fluid) . VOF 2
 가 2
 . VOF [10]

VOF 가 (fixed grid system)
 . VOF
 (volume fraction)

VOF 가
 가 (phase)
 가 (volume fraction)
 (control volume) (sum) 1(unity)
 (variables and properties)
 (volume averaged values)

(cell)
 , (mixture)
 q ,
 α_q 가 가 가 .

$\alpha_q = 0$ the cell is empty (of the q th fluid)
 $\alpha_q = 1$ the cell is full (of the q th fluid)
 $0 < \alpha_q < 1$ the cell contains the interface between the fluids

α_q 가
 (phase) (interface) 가 ()
 (continuity equation) . q
 :

$$\frac{\partial \alpha_q}{\partial t} + u_i \frac{\partial \alpha_q}{\partial x_i} = S_{\alpha_q} \quad (1)$$

source term VOF model 0(zero)
 1 (primary phase)

$$\sum_{q=1}^n \alpha_q = 1 \quad (2)$$

1 2

cell

$$\rho = \alpha_2 \rho_2 + (1 - \alpha_2) \rho_1 \quad (3)$$

N 가

$$\rho = \sum \alpha_q \rho_q \quad (4)$$

VOF model

cell 가

$\rho \quad \mu$

$$\frac{\partial}{\partial t} \rho u_j + \frac{\partial}{\partial x_i} \rho u_i u_j = - \frac{\partial P}{\partial x_j} + \frac{\partial}{\partial x_i} \mu \left(\frac{\partial u_i}{\partial x_j} + \frac{\partial u_j}{\partial x_i} \right) + \rho g_j + F_j \quad (5)$$

4. Sparger

sparger IRWST

‘I’ sparger 가 Fig. 7
(LRR; Load Reduction Ring), 10 mm 가 144 25

mm 가

Figure 8 sparger IRWST outline 2

LRR sparger head Sparger head
9

3 (discharge coefficient)

LRR

sparger head , sparger head
sparger head

가

sparger head
LRR

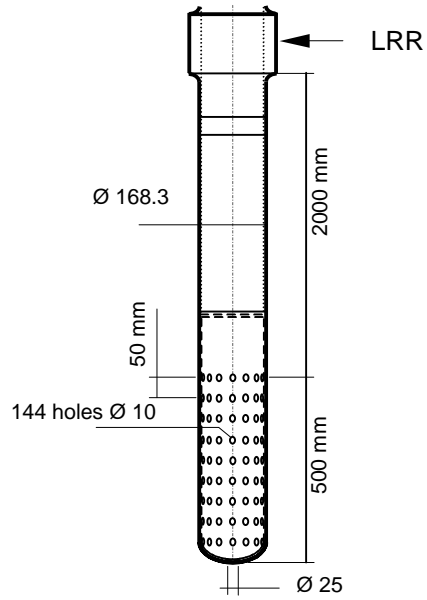


Fig. 7 Schematic of I-type sparger.

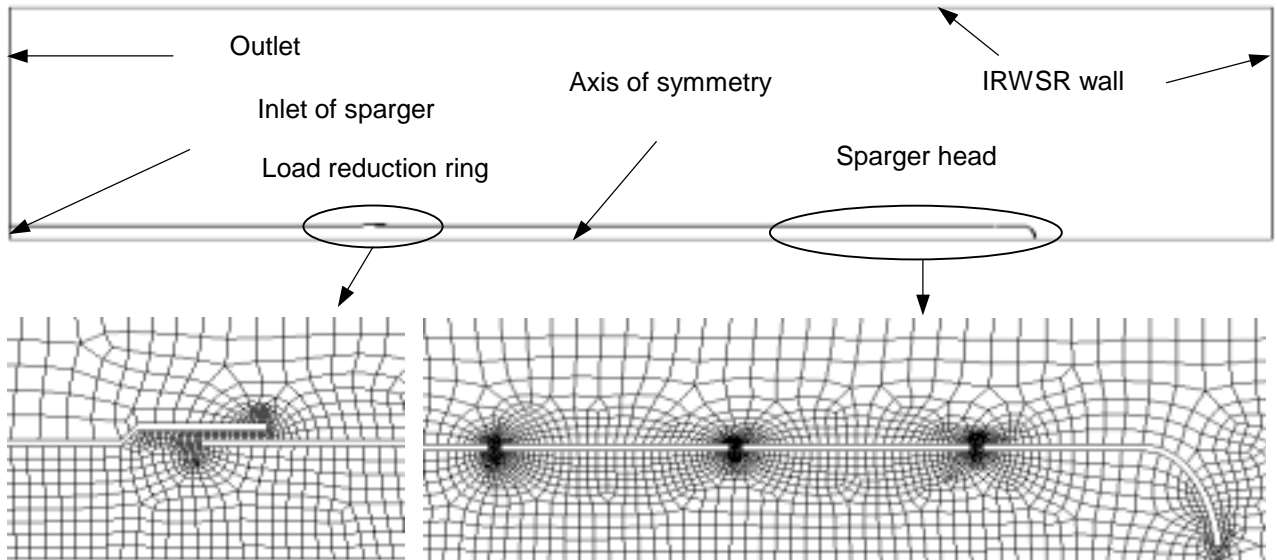


Fig. 8 Outline and grid for I-type sparger.

sparger header

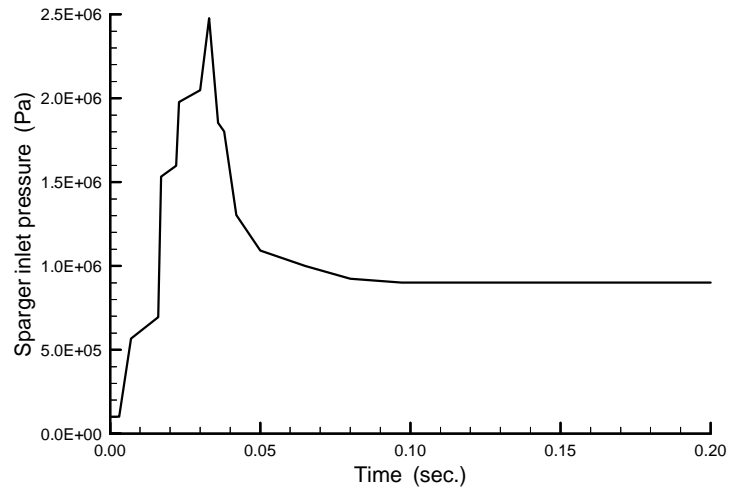


Fig. 9 Pressure history at the inlet of a sparger.

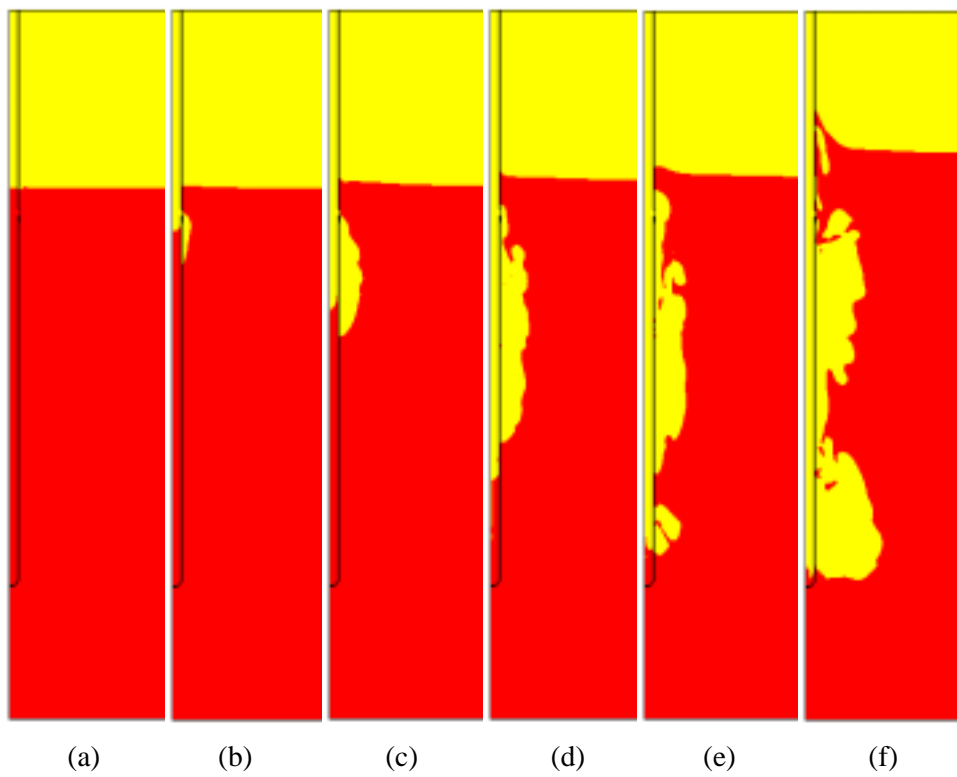


Fig. 10 The shape of the bubble during air discharge (a) Time = 0.0 sec, (b) Time = 0.0325 sec, (c) Time = 0.060 sec, (d) Time = 0.130 sec, (e) Time = 0.170 sec, (f) Time = 0.270 sec.

Figure 10

LRR sparger head

Figure 10

Figure 11 LRR

sparger head IRWST

가

POSRV

(shock wave)

sparger header

(Fig. 9) LRR

IRWST

LRR

IRWST

가

LRR

IRWST

가

가

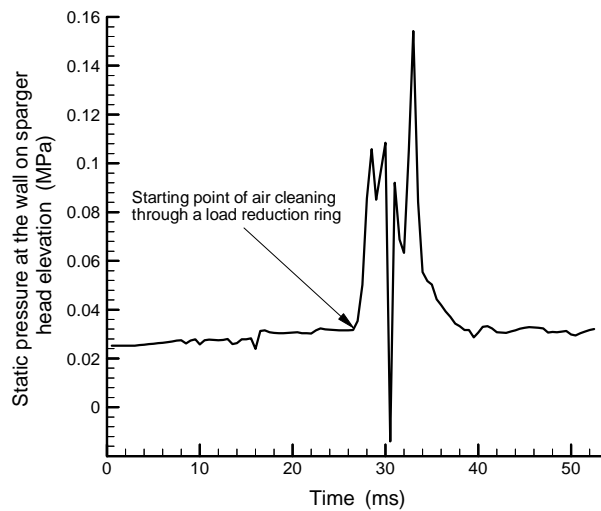


Fig. 11 IRWST wall pressure on sparger head elevation during air cleaning through a load reduction ring.

LRR

IRWST

가

Figure 12(a)

LRR sparger head

IRWST

Figure 12(b)~(d) LRR

IRWST

IRWST

LRR sparger head

IRWST

IRWST

IRWST

Fig. 12(b)

가 . Figure 1

50 m/s 가

가 , 가

1570 m/s 가
(hammering)

IRWST 가 sparger header LRR

IRWST

, IRWST (pressure oscillation) 가

. LRR IRWST

IRWST . IRWST

sparger head IRWST sparger tube 가 ,

(Fig. 11) .

FLUENT

IRWST

IRWST

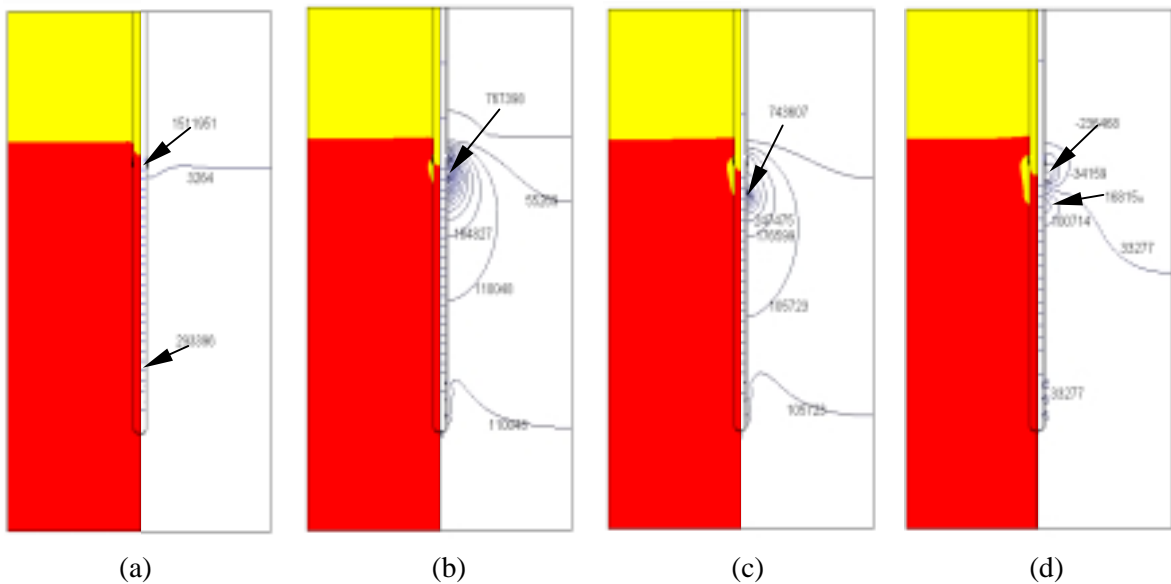
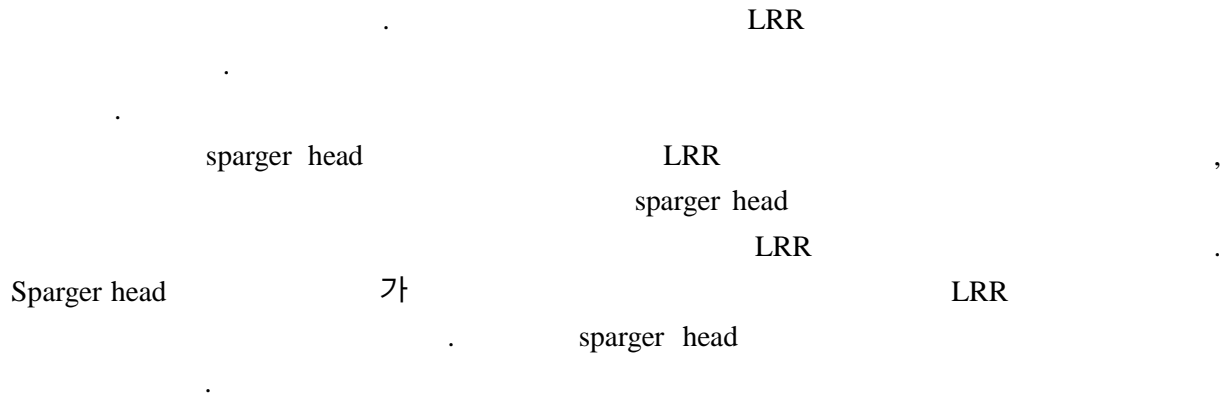
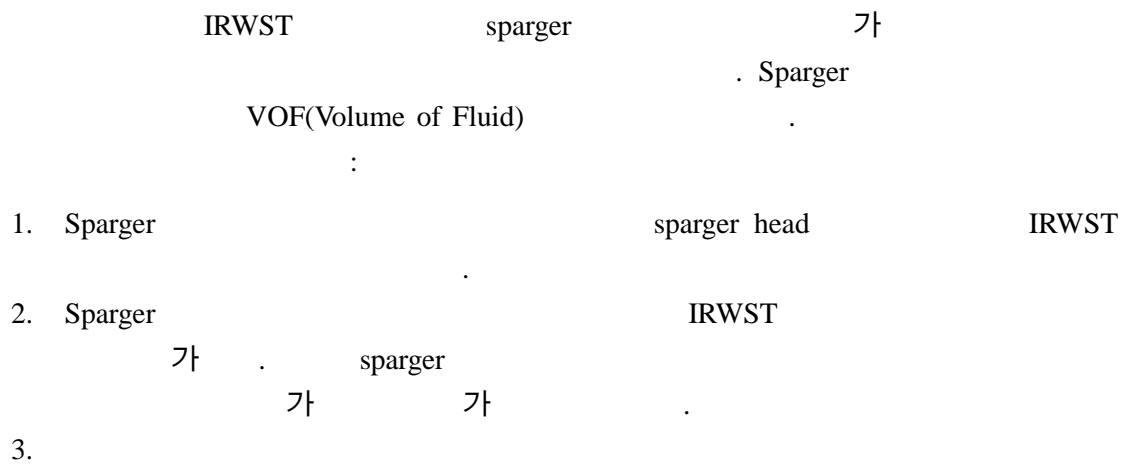


Fig. 12 Pressure distribution during water and air discharge (Pa), (a) Time = 0.002 sec, (b) Time = 0.0325 sec, (c) Time = 0.035 sec, (d) Time = 0.0375 sec.

Fig. 12(d)



5.



[1] F. Yamamoto, M. Iguchi, J. Ohta, and M. Koketsu, "Measurement of Bubbling-Jet Two-Phase Flow Using 3-D PTV Based on Binary Image Cross-Correlation Method", FED-Vol. 209, *Flow Visualization and Image Processing of Mutiphase Systems*, pp. 131-136, 1995.

[2] Y. Murai and Y. Matsumoto, "Three Dimensional Structure of a Bubble Plume – Measurement of the Three Dimensional Velocity", FED-Vol. 209, *Flow Visualization and Image Processing of Multiphase Systems*, pp. 187-194, 1995.

[3] M.E. Simpson and C.K. Chan, "Hydrodynamics of a Subsonic Vapor Jet in Subcooled Liquid", *J. Heat Transfer*, Vol. 104, pp. 271-278, 1982.

- [4] L-D. Chen and G.M. Faeth, "Condensation of Submerged Vapor Jets in Subcooled Liquids", *J. Heat Transfer*, Vol. 104, pp. 774-780, 1982.
- [5] J.C. Weimer, G.M. Faeth, and D.R. Olson, "Penetration of Vapor Jets Submerged in Subcooled Liquids", *AIChE Journal*, Vol. 19, No. 3, pp. 552-558, 1973.
- [6] H. Luo and H. Svendsen, "Theoretical Model for Drop and Bubble Breakup in Turbulent Dispersions", *AIChE Journal*, Vol. 42, No. 5, pp. 1225-1233, 1996.
- [7] M.J. Prince, and H.W. Blanch, "Bubble Coalescence and Break-Up in Air-Sparged Bubble Columns", *AIChE Journal*, Vol. 36, No. 10, pp. 1485-1499, 1990.
- [8] I. Tiselj And S. Petelin, "Modelling of Two-Phase Flow with Second-Order Accurate Scheme", *J. Computational Physics*, Vol. 136, pp. 503-521, 1997.
- [9] C.W. Hirt and B.D. Nichols, "Volume of Fluid (VOF) Method for the Dynamics of Free Boundary", *J. Computational Physics*, Vol. 39, pp. 201-225, pp. 1981.
- [10] FLUENT Inc., "FLUENT manual, User's Guide", 1998.
- [11] J.K. Park, K.J. Ryu, Y.S. Shim, Y.S. Kim, K.Y. Lee, J. Lee, and Y.I. Kim, "The Analysis of the Characteristics of Steam Condensation and Thermal Mixing inside IRWST and Flow through Pressurizer Discharge Pipe", *Technical Report, KAERI/TR-609/95*, Korea, 1995.